International Journal of Heat and Mass Transfer 52 (2009) 3984–3993

Contents lists available at ScienceDirect

International Journal of Heat and Mass Transfer

journal homepage: www.elsevier.com/locate/ijhmt

# Analysis of convective two-phase flow instabilities in vertical and horizontal in-tube boiling systems

Sadık Kakaç [a,*], Liping Cao [b]

[a] TOBB University of Economics and Technology, Ankara, Turkey
[b] Westinghouse Electric Company, LLC, Monroeville, PA 15146, USA

ARTICLE INFO

*Article history:*
Received 13 January 2009
Accepted 23 March 2009
Available online 4 May 2009

*Keywords:*
Two-phase flow
Dynamic boiling instabilities
Drift-Flux model

ABSTRACT

In this work, analysis of two-phase flow boiling instabilities in vertical and horizontal systems is presented. The steady-state system pressure-drop characteristics are determined by a numerical solution of the governing equations as derived from the Drift-Flux model. The transient characteristics of the two-phase flow are obtained for various parameters and the results are presented in graphical and tabular forms. The numerical solutions are determined using an explicit finite difference scheme. The results of numerical solutions are verified by the experimental findings. A satisfactory agreement between the theory and experiments is obtained.

© 2009 Elsevier Ltd. All rights reserved.

## 1. Introduction

Two-phase instabilities have been observed to occur in many industrial domains like refrigeration systems, turbo-machinery, boiling water reactors, and two-phase flow heat exchangers. Predictions of flow parameters such as steady-state pressure-drop characteristics, stability boundaries during boiling, and oscillations are very crucial in the design and operation of two-phase flow equipment. Thermal oscillations are undesirable as they can cause problems of system control, and can lead to the failure of the tube caused by a continuous cycling of the wall temperature. It is clear from these problems that plant equipment should posses an adequate margin of safety against oscillations. There have been many analytical and experimental investigations on the two-phase flow instability as can be found in the review papers by Bouré et al. [1], Bergles [2], Lahey and Drew [3], Yadigaroglu [4], Kakaç and Liu [5], Kakac and Bon [6], Stenning [7], and Stenning and Veziroglu [8] investigated and identified three types of dynamic instabilities, namely, density-wave type, pressure-drop type, and thermal oscillations, in a single channel up flow boiling system.

Convective subcooled boiling has been receiving special attention since four decades by researchers over the world, some of the relevant works on the subject are Maulbetsch [9], Zuber et al. [10], Zuber and Dougherty [11], Kroeger and Zuber [12], and Saha and Zuber [13]. In these works, several correlations were presented corresponding to different range of operating conditions and working fluid.

The objective of this work is to study theoretically and experimentally the steady-state and oscillatory characteristics of flow boiling in a single vertical and horizontal tubes. The Drift-Flux model is used for prediction of steady-state characteristics and the pressure-drop type instabilities with upstream compressible volume introduced through a surge tank.

## 2. Experimental apparatus

### 2.1. Description of the system

Figs. 1 and 2 are schematic diagrams of the upflow and horizontal boiling systems used in the experimental study. Two systems components are the same except for the test section. The test fluid, the refrigerant, is supplied from the liquid container pressurized by nitrogen gas. A thermostatically controlled immersion heater in the liquid container and a cooling unit before the test section provide an inlet temperature range of −20 to 90 °C, with a control accuracy of ±1.0 °C. Following the 60.5 cm long electrically heated test section is a recovery section consisting of a condenser and a collector tank. The mixture of saturated liquid and vapor is led through the condenser coil, which is cooled by refrigerated brine at 0 °C. The condensed liquid is then stored in a recovery tank that is maintained at a constant pressure to ensure constant levels of container and exit pressure.

All the tubing, except the recovery section, is made of 0.75 cm (0.295 in.) ID nichrome tube. The surge tank, which is an important dynamic component of the system, provides the necessary compressible volume for the pressure-drop type oscillations to occur. Appropriate instrumentation is installed to provide control and measurements of the test parameters, namely, flow rate, pressure,

* Corresponding author.
*E-mail address:* sadikkakac@yahoo.com (S. Kakaç).

0017-9310/$ - see front matter © 2009 Elsevier Ltd. All rights reserved.
doi:10.1016/j.ijheatmasstransfer.2009.03.025

**Nomenclature**

| | |
|---|---|
| $A_c$ | cross-sectional area |
| $d_e$ | effective diameter |
| $d_i$ | diameter of the exit restriction |
| $D_i$ | inner diameter of the tube |
| $C_0$ | distribution parameter |
| $C_s$ | dimensionless surface coefficient |
| $c_1$ | coefficient in the exit restriction model [Eq. (1)] |
| $c_2$ | coefficient in the exit restriction model [Eq. (1)] |
| $c_p$ | specific heat |
| $D_h$ | diameter of the heater |
| $f_f$ | single-phase liquid friction factor |
| $f_m$ | two-phase mixture friction factor |
| $g$ | acceleration due to gravity (9.806 m/s$^2$) |
| $G$ | mass velocity |
| $h$ | local heat transfer coefficient |
| $h_{lv}$ | latent heat of evaporation |
| $i$ | enthalpy |
| $j$ | volumetric flux |
| $k$ | velocity ratio, $u_g/u_l$ |
| $k_l$ | saturated liquid thermal coefficient |
| $K_i$ | inlet orifice coefficient (from main tank to surge tank) |
| $L_0$ | length of the channel |
| $L_i$ | length of the tube from main to surge tank |
| $\Delta l$ | axial length along heated section |
| $\dot{m}$ | mass flow rate |
| Nu | Nusselt number, $hd_e/k_l$ |
| $P$ | pressure |
| $\Delta P$ | pressure-drop |
| $P_e$ | exit pressure |
| $P_c$ | critical pressure |
| $P_s$ | surge tank pressure |
| $P_t$ | surge tank pressure |
| $P_{tv}$ | vapor partial surge tank pressure |
| Pe | Peclet number, $GD_hc_{p,f}/k_f$ |
| $P_{ta0}$ | steady-state pressure of air in the surge tank |
| $q$ | heat flux density |
| $Q_l$ | heat input into the fluid |
| $Q_0$ | rate of electric heat generations in the tube |
| $t$ | time |
| $T$ | temperature |
| $u$ | fluid velocity |
| $u_i$ | liquid inlet velocity in the surge tank |
| $u_o$ | liquid outlet velocity in the surge tank |
| $V_{a0}$ | volume of air in surge tank at steady state |
| $V_{gj}$ | drift velocity of vapor |
| $x$ | vapor quality |

*Greek symbols*

| | |
|---|---|
| $\alpha$ | void fraction |
| $\beta$ | exit restriction diameter ratio, $d_i/D_i$ |
| $\Gamma_g$ | mass rate of vapor generation per unit volume |
| $\mu$ | dynamic viscosity of the fluid |
| $\rho$ | density |
| $\xi_h$ | heated perimeter |
| $\sigma$ | surface tension |

*Subscripts*

| | |
|---|---|
| $eq$ | equilibrium assumption |
| $f$ | liquid phase |
| $g$ | vapor phase |
| $i$ | inlet |
| $h$ | heater |
| $l$ | liquid |
| $l_0$ | liquid alone with the mass flow rate of the total two-phase flow |
| $s$ | steady state |
| $t$ | tank |
| $tp$ | two-phase |
| $w$ | wall |

and temperature at various locations and the electrical heat input. Further discussion and details of the experimental set-up can be found elsewhere [5,14,15,16,17].

### 2.2. Experimental procedure

For a given heater tube, different sets of experiments, corresponding to various heat inputs, have been conducted. For each heater tube, an initial experiment is conducted without any heat input, to determine the single-phase characteristics. Each set is composed of a sufficient number of tests to cover the available flow range. Stability boundaries have been determined in each case. Oscillations have been identified by the cyclic variations in pressures and flow rates, by observing recordings. In defining the stability boundary, short life transients have been disregarded, and only sustained oscillations have been considered.

The procedure for the actual tests can be outlined as follows:

(1) With enough liquid in the container tank, the tank is pressurized by using nitrogen gas.
(2) The surge tank is half-filled with Freon 11 and pressurized to a predetermined value by compressed air.
(3) The flow rate and the heat input are increased gradually to the desired starting point, and the system is allowed to become steady, as indicated by the recordings of system pressures, temperatures, and flow rate.
(4) Measurements of temperatures, pressures, flow rate and heat input, and critical observations are noted.
(5) The mass flow rate is reduced by a small amount using the inlet control valve, and the system is allowed to become steady before the readings are noted down.

This procedure is repeated starting at step (4) until sustained oscillations are observed. After reaching the unstable region, the mass flow rate is first increased into the stable region and then decreased in small steps to precisely locate the instability boundary.

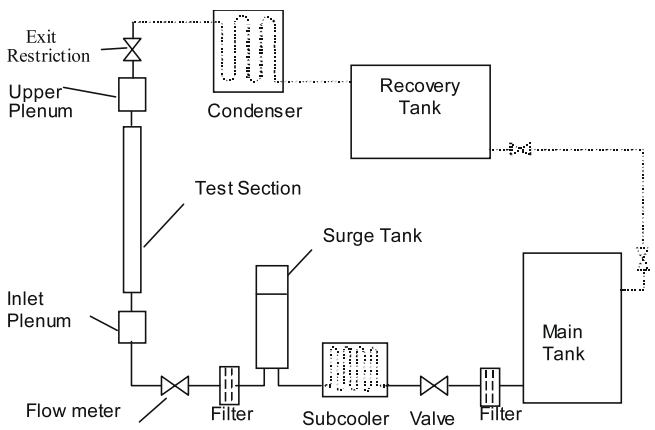


**Fig. 1.** Schematic diagram of the vertical experimental system.

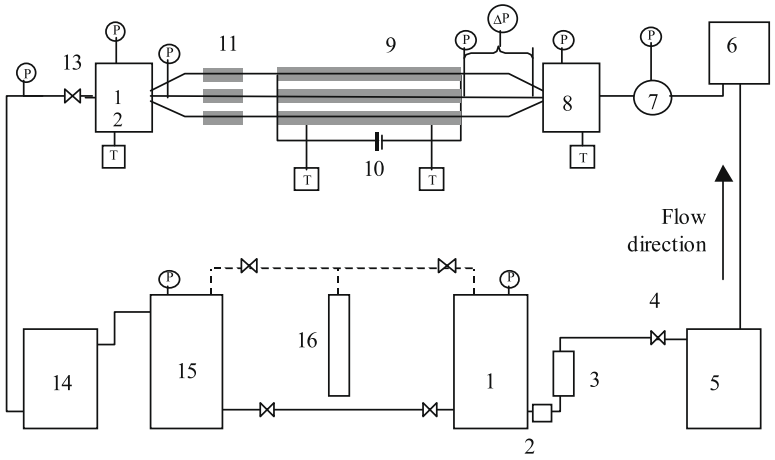


**Fig. 2.** Schematic diagram of the horizontal experimental set-up.

(6) While operating in the unstable region, first the heater inlet pressure and temperature are recorded. Then, the system is stabilized by closing the inlet-throttling valve slowly. After taking the readings, the inlet valve is brought into fully open position, and the mass flow rate is further reduced by a small amount.

Following each adjustment, the system is allowed to stabilize, and the procedure is continued. The experiment is stopped after the dry-out point is reached. Further details of the experimental procedure can be found in [16,18].

## 3. Mathematical modeling of the exit restriction

The throttling sharp-edged orifice is located at the exit of the test heater. It is an essential component to generate the two-phase flow dynamic instabilities in a boiling flow system. The generating mechanism of the pressure-drop type oscillations in a boiling two-phase flow system is the pressure-drop mass flow rate steady-state characteristics of the system. So, the exit restriction needs to be modeled with acceptable accuracy and reliability in the first place, in order to come to a successful description of the whole system. Both the steady-state performance and the dynamic response of such systems depend on, for the most part, the pressure-drop of fluid flowing through this exit restriction at specific mass flow rate and mass quality of the gas–liquid mixture. The earlier experimental study, Liu [18] has shown that about 90% of the system pressure-drop is concentrated in the exit restriction orifice.

In the previous studies [14–16,18,19] of the system dynamic instabilities with our experimental set-up, purely empirical correlations were given in the form of pressure-drop as an approximate polynomial of quality $x$ through the exit restriction, based on the experimental values.

Theoretical models for two-phase mixture flowing through the orifice have all been based on either homogeneous or separated flow model that simulates ideal cases of two-phase mixture flow. The homogeneous model considers the two phases to flow as a single phase with mean fluid properties, while separated model considers the phases to be artificially segregated into two streams: one of liquid and one of vapor. However, in reality, experiments showed that the flow at the throat of an orifice was neither exactly homogeneous nor wholly separated, so the models were all modified to correlate the experimental data in applications. The exit restriction is a sharp-edge orifice located at the outlet of the heater, with diameter of 2.64 mm.

The following correlation was developed, Eq. (1) by modifying the separated flow model of two-phase fluid flowing through the orifice Cao [20] and Cao et al. [21]:

$$\frac{\Delta P_{tp}}{\Delta P_{lo}} = 1 + \left(\frac{v_g}{v_l} - 1\right) c_1 x^{c_2} \tag{1}$$

The constants $c_1$ and $c_2$ are obtained by correlating the experimental results. It is found that $c_1$ increases with the heat input, while $c_2$ is kept constant (see Table 1). This correlation is the modified version of the Chisholm's correlation, Chisholm [22]. Fig. 3 shows the exit restriction model and experimental measurements at various heat inputs.

## 4. Steady-state characteristics

Mathematical representation of the experimental systems are shown in Figs. 4 and 5, for vertical and horizontal systems, respectively, where five distinct regions are identified along the system, each having different characteristics.

The components upstream of the inlet of the heated channel are lumped together and considered as the first region. The whole length of the heater is divided into the subcooled liquid region and the boiling two-phase fluid region, which are numbered as

**Table 1**
$c_1$ and $c_2$ for different heat inputs.

| Heat input (W) | $c_1$ | $c_2$ |
|---|---|---|
| 1000 | 2.4 | 1.5 |
| 800 | 2.3 | 1.5 |
| 600 | 1.5 | 1.5 |
| 400 | 1.0 | 1.5 |

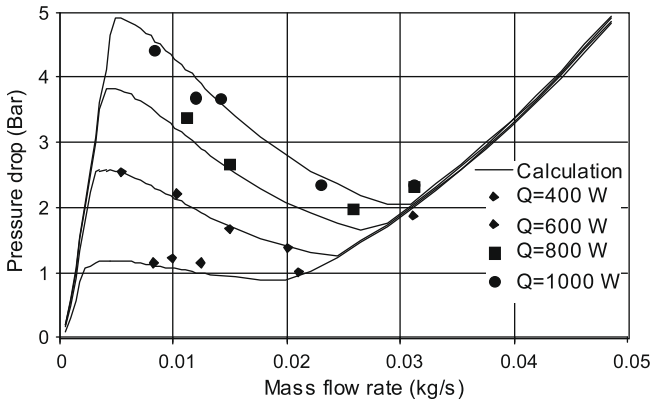


**Fig. 3.** Steady-state characteristics of exit restriction. Comparison of the present model with experimental data [21].

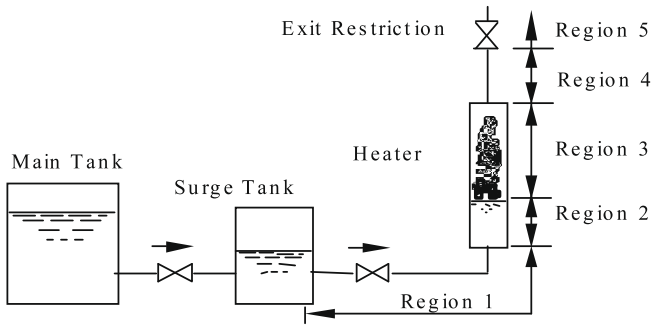


**Fig. 4.** Mathematical model representation of the vertical system.

the second and third region. Region 4 extends from the exit of the heater to the exit restriction. The restriction exit is treated separately as region 5 (Figs. 4 and 5).

### 4.1. Single-phase liquid region

The liquid is considered to be incompressible and one-dimensional with constant thermodynamic and transport properties. Therefore, the conservation equations are [15,21,23]:

(1) Continuity

$$\frac{\partial u_f}{\partial z} = 0 \tag{2}$$

(2) Momentum

$$\rho_f u_f \frac{\partial u_f}{\partial z} = -\frac{\partial P}{\partial z} - \frac{f_f}{2D_h}\rho_f u_f^2 + g\rho_f \tag{3}$$

(3) Energy

$$u_f \frac{\partial i_f}{\partial z} = \frac{q_w \xi_h}{\rho_f A_c} \tag{4}$$

### 4.2. Two-phase mixture region

Drift-Flux model is used to formulate the problem in the two-phase mixture region. The time-smoothed, one-dimensional conservation equations as derived by Ishii [24] are:

(1) Conservation of mass of the mixture

$$\frac{\partial(\rho_m u_m)}{\partial z} = 0 \tag{5}$$

(2) Conservation of mass of the vapor phase

$$\frac{\partial(\alpha\rho_g u_g)}{\partial z} = \Gamma_g \tag{6}$$

(3) Conservation of momentum of the mixture (neglecting the effect of surface tension)

$$\rho_m u_m \frac{\partial u_m}{\partial z} = -\frac{\partial P_m}{\partial z} - \frac{f_m}{2D_h}\rho_m u_m^2 + g\rho_m - \frac{\partial}{\partial z}\left(\frac{\rho_f - \rho_m}{\rho_m - \rho_g}\frac{\rho_f \rho_g}{\rho_m} V_{gj}^2\right) \tag{7}$$

(4) Conservation of energy of the mixture (neglecting the effect of the kinetic and potential energy)

$$\rho_m u_m \frac{\partial i_m}{\partial z} = \frac{q_w \xi_h}{A_c} - \frac{\partial}{\partial z}\left(\frac{\rho_f - \rho_m}{\rho_m}\frac{\rho_f \rho_g}{\rho_f - \rho_g} V_{gj}(i_g - i_f)\right) \tag{8}$$

The mixture density, $\rho_m$; the mixture pressure, $P_m$; the mixture velocity, $u_m$; and the mixture enthalpy, $i_m$; are defined as:

$$\rho_m = \alpha\rho_g + (1-\alpha)\rho_f \tag{9}$$

$$P_m = \alpha P_g + (1-\alpha)P_f \tag{10}$$

$$u_m = \frac{\alpha\rho_g u_g}{\rho_m} + \frac{(1-\alpha)\rho_f u_f}{\rho_m} \tag{11}$$

$$i_m = \frac{\alpha\rho_g i_g}{\rho_m} + \frac{(1-\alpha)\rho_f i_f}{\rho_m} \tag{12}$$

Instead of solving the problem in a general form, the following simplification assumption is introduced:

(1) There is no pressure difference between the phases.

$$P_m = \alpha P_g + (1-\alpha)P_f = P = P_f = P_g \tag{13}$$

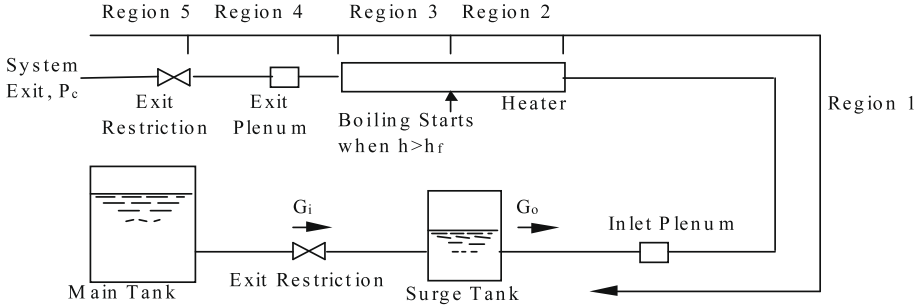


**Fig. 5.** Mathematical model representation of the horizontal system.

(2) The enthalpy of the vapor phase is a constant and is equal to the corresponding saturation value.
(3) Liquid phase is incompressible.

### 4.3. The kinematic correlation for void fraction

The model used in the present study was proposed by Zuber and Findlay [25]. According to their analysis, the vapor velocity, $u_g$, is related to the volumetric flux as:

$$u_g = C_0 j + V_{gj} \tag{14}$$

where $C_o$ is the distribution parameter, $V_{gj}$ is the drift velocity of the vapor phase with respect to the center of mass of the mixture and $j$ is the volumetric flux defined as

$$j = u_l(1-\alpha) + u_g\alpha \tag{15}$$

The following expressions are reported to give good results for steam-water flows irrespective of the flow pattern [25].

$$C_0 = 1.41 \tag{16}$$

$$V_{gj} = 1.41\left[\frac{\sigma g(\rho_l - \rho_g)}{\rho_l^2}\right]^{1/4} \tag{17}$$

### 4.4. Solution of the steady-state characteristics

The conservation equations, together with the equations of state and the constitutive relations, are to be solved for the following boundary conditions:

- constant inlet temperature, $T_i$ constant,
- constant heat input, $Q_l$ constant and uniform,
- constant exit pressure, $P_e$ constant.

The governing equations, outlined earlier, are discretized in the space coordinate to solve for the steady-state characteristics of the system. Calculations start with given values of mass velocity $G$, fluid inlet temperature $T_i$, heat input $Q_l$, and exit pressure $P_e$. Assuming an inlet (surge tank) pressure $P_s$, the flow parameters and properties are calculated from the exit of the surge tank to the inlet of the heater. The enthalpy, pressure, and density are calculated at each successive node in the heater. Without considering the subcooled boiling effect, the starting point of boiling is assumed to be the point where the bulk liquid temperature reaches the saturation temperature corresponding to the local pressure. The whole length of heater is divided by the boiling point into the single-phase section and two-phase boiling section. These sections are computed using their respective finite difference forms of the governing equations using appropriate state and constitutive equations according to the state of the fluid. The calculation is carried out from the surge tank to the system exit by matching process in the space coordinate. The trial and error method is used by assuming different value of $P_s$ to arrive at the given value of $P_e$ within given errors. But in a real system, however, will not be in thermodynamic equilibrium, because the vapor bubble generation starts while the liquid bulk temperature is very much below the saturation temperature with high local subcooling. After the point of net vapor generations, the liquid bulk temperature beyond this point is lower than that predicted by thermal equilibrium, because part of the heat added to the system is used to generate vapor, and the quality; in the present analysis, this region is called thermodynamically, non-equilibrium model and is considered in the analysis of dynamic oscillations.

The steady-state characteristic curves of the system are shown in Figs. 6 and 7, as comparisons of the model calculations with the experiments. In Fig. 6, different curves corresponding to the different heat inputs are shown, while Fig. 7 presents different inlet subcoolings of the fluid. As the steady-state characteristics also determine the stability boundaries and dynamic characteristics of the quasi-steady pressure-drop type oscillations, the neglecting of the subcooled boiling will also cause errorness in the theoretical prediction of the stability boundaries and the oscillation characteristics, as will be shown in following sections.

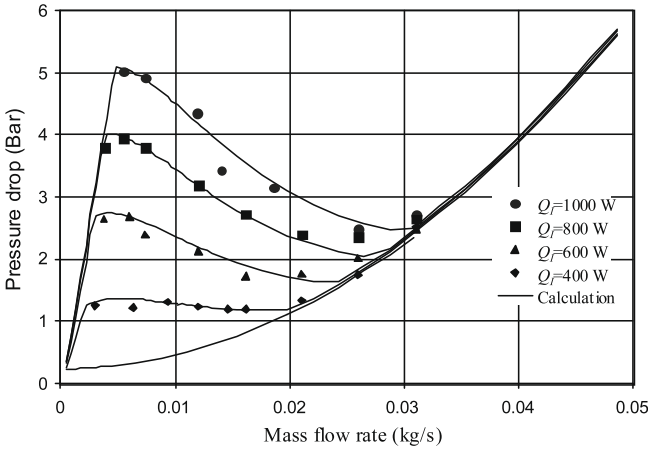


**Fig. 6.** Vertical system steady-state characteristics with different heat input ($T_i$ = 23 °C) [21].

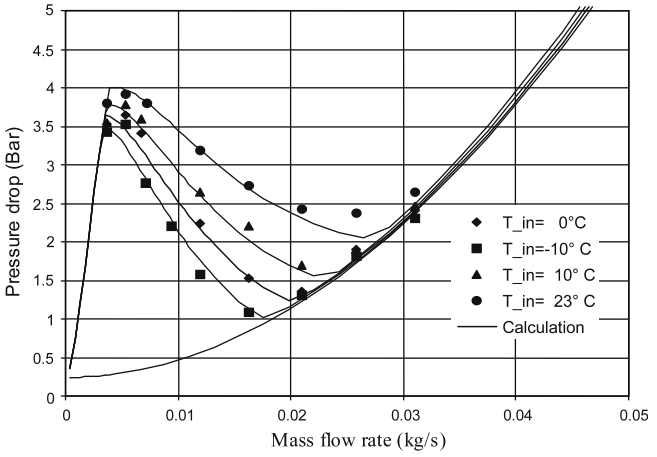


**Fig. 7.** Vertical system steady-state characteristics with different inlet subcooling ($Q$ = 800 W) [21].

### 4.5. Model of the pressure-drop type oscillations

Pressure-drop type oscillations that occur in two-phase flow systems are triggered by a small instability in the negative slope region of the steady-state characteristic curve. The surge tank is an important dynamic component of the system that serves as an "external compressible volume". The oscillations have relatively low frequencies, and their periods are usually much longer than the residence time of a single fluid particle in the system. Consequently, quasi-static condition is assumed in modeling the pressure-drop type instability in the boiling system, which means the transient operating points can be obtained as a series of steady-state points. In addition, the following assumption about the physical system is made to form the present dynamic model:

(1) The temperature inside the surge tank is constant during oscillations.

(2) The heat input to the fluid is constant during the oscillations, i.e., the dynamics of the heater wall is neglected.

For surge tank, the continuity equation can be written as [19,21]:

$$\frac{dP_t}{dt} = \frac{(P_t - P_{tv})^2 A_c}{P_{ta0} V_{a0}} (u_i - u_o) \tag{18}$$

The momentum equation between the main tank and the surge tank is written as:

$$\frac{du_i}{dt} = \frac{1}{\rho_l L_i} [(P_i - P_t) - K_i \rho_l u_i^2] \tag{19}$$

where $K_i$ is the inlet restriction coefficient of the valve between the main and surge tanks.

With the quasi-static assumption of during the pressure-drop type oscillation, the momentum equation between the surge tank and the system exit can be written as:

$$\frac{du_o}{dt} = \frac{1}{\rho_l L_o} [(P_t - P_e) - (P_t - P_e)_s] \tag{20}$$

where $(P_t - P_e)_s$ is the steady-state pressure-drop given in the earlier section.

Eqs. (18)–(20) form the dynamic model of the system under the pressure-drop type oscillation. The 4th order Runge–Kutta method is used with the MATLAB software to numerically solve the pressure-drop oscillation.

### 4.6. Solutions to the model

#### 4.6.1. Stability boundaries of the system

The stability boundaries of the system are obtained by varying the mass flow rate under given heat input and inlet subcooling in the nonlinear dynamic simulations.

Small pressure perturbation to the surge tank pressure is imposed to the system under steady state of the different operating conditions, and the time process of the parameter variation of the perturbed system is traced in the simulation to determine the point where the oscillations start. Stable system returns back to the steady state under perturbation, while the unstable system presents limit cycle of the pressure and mass flow rate variation with time.

The system stability boundary is determined in the steady-state pressure-drop versus mass flow rate plane, as shown in Fig. 8. The experimental data on the onset of flow oscillation corresponding to various heat inputs are compared with the results of model calculation in Fig. 8. As can be seen clearly in the figure, the theoretical and experimental results fit fairly well Cao [20] and Cao et al. [21].

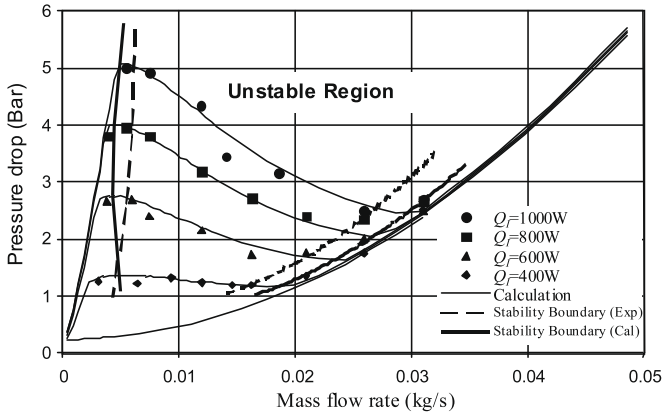


**Fig. 8.** Stability boundaries.

### 4.7. Nonlinear simulations of the pressure-drop oscillations

Initial values of the steady state of the system plus the perturbation to the system also need to be included before obtaining the simulation results of the system oscillations.

The time variations of the surge tank pressure and mass flux of the system predicted by the theoretical models are presented in Tables 2 and 3 [20]. These two tables correspond to different heat inputs, and inlet subcoolings $Q$ and mass flow rate ($\dot{m} = 11.89$ g/s). For comparison between the theoretical predictions with the experiments, the experimental recordings of the inlet pressure oscillations are included in these tables.

It is seen from these tables, first, that the periods of the oscillations are reasonably well predicted by the dynamic model presented. The higher the heat flux, the larger the periods of the oscillation, which is expected as the slope of the negative parts of steady-state curve (Fig. 6) becomes steeper as the heat input into the system increases. The steeper the negative slope, the more unstable the system becomes (Fig. 8).

Under different heat inputs and inlet fluid temperatures, the comparison of the non-equilibrium to the equilibrium models in predicting the oscillation periods are listed in the Tables 2 and 3 for the vertical system. The results are grouped in Tables 2 and 3 for inlet temperatures $T_i = 23$, 10, 0, and $-10$ °C. Neglecting the subcooled boiling contributes to the errorness of the prediction of the oscillation characteristics (period and amplitude).

The equilibrium model always results in larger period comparing with that resulted from non-equilibrium model, due to the delay of boiling threshold and consequently, the negative slope region on the steady-state characteristic curves of the boiling system.

In Tables 2 and 3 it can be seen that, when the inlet fluid temperature decreases, the heat input has different effect on the oscillating period. The oscillating period first increase with the increase of heat input from $Q_l = 400$–$1000$ W in Table 2 when $T_i = 23$ °C; then the heat input has little effect on the period when $T_i = 10$ °C; finally when $T_i = 0$ and $-10$ °C, the period decreases as heat input increases.

**Table 2**
Comparison of experimental and theoretical results of pressure-drop oscillations. (Bare tube; tube I.D. = 7.5 mm; exit restriction = 1.6 mm; $\dot{m} = 11.89$ g/s).

| Temperature (°C) | Heat input (W) | Theoretical (non-equilibrium) period (s) | Theoretical (equilibrium) period (s) | Experimental (Liu [18]) period (s) |
|---|---|---|---|---|
| 23 | 400 | 14.2 | 15.1 | 13.5 |
| | 600 | 17.2 | 21.0 | 17.0 |
| | 800 | 31.5 | 36.8 | 28.5 |
| | 1000 | 38.0 | 51.5 | 32.5 |

**Table 3**
Comparison of theoretical results of pressure-drop oscillations for a vertical tube. (Bare tube; tube I.D. = 7.5 mm; exit restriction = 1.6 mm; $\dot{m} = 11.89$ g/s).

| Temperature (°C) | Heat input (W) | Theoretical (non-equilibrium) period (s) | Theoretical (equilibrium) period (s) |
|---|---|---|---|
| 10 | 600 | 38.2 | 44.7 |
| | 800 | 37.3 | 45.2 |
| | 1000 | 35.8 | 44.6 |
| 0 | 600 | 50.4 | 56.0 |
| | 800 | 48.4 | 54.8 |
| | 1000 | 43.1 | 52.4 |
| −10 | 600 | 67.5 | 71.0 |
| | 800 | 58.4 | 66.9 |
| | 1000 | 51.8 | 60.7 |

It can also be seen from Tables 2 and 3 that the differences of oscillating periods between the non-equilibrium and equilibrium models vary with the heat input and inlet temperature values.

### 4.8. Model of thermal oscillations

The phenomenon of thermal oscillations induced by two-phase flow is of importance for the design and operation of many industrial systems and equipments such as steam generators, thermosiphon reboilers, refrigeration plants, and various heat exchangers used in chemical processes units and refineries. The understanding of pressure-drop and density-wave type two-phase flow instability mechanisms is now essentially complete; some relevant work on the dynamic of two-phase flow boiling systems concerning pressure-drop and density-wave oscillation and the mathematical modeling of are cited in Bergles [2] and Bouré et al. [1].

The experimental study, as well as analytical model, of thermal oscillations remains limited for two reasons. First, the understanding of two-phase flow heat transfer in steady state is rather limited; second, the theoretical aspects of unsteady and oscillatory phenomena in convective heat transfer are not fully clarified yet. As the state-of-the-art on these fronts keeps developing, phenomena such as the one described in this work will be understood completely. Thus, the study of thermal oscillations is important for practical, as well as scientific, reasons.

In our experimental studies, thermal oscillations were observed, in addition to pressure-drop and density-wave oscillations. These are dynamic oscillations, accompanied by large fluctuations in temperature. The flow oscillates between low quality (dryness fraction) and high quality regions at a given point in the heater. The wall superheated fluctuates correspondingly to accommodate the constant heat generation in the wall, as the heat conditions. Kakaç et al. [14] and Padki et al. [15] presented experimental and theoretical investigations on thermal oscillations. The theoretical modeling was carried out under the assumption of homogenous flow and thermodynamic equilibrium between the vapor and liquid phases. In this paper, some further work on the modeling of pressure-drop type and thermal oscillations is presented.

Experiments have been carried out with two vertical nicrome tubes (7.5 mm inner diameter and 9.5 mm outer diameter) – one bare and the other coated with Linde High Flux coating – at various heat inputs (0, 400, 600, 800, and 1000 W), keeping the inlet fluid temperature constant at room temperature. In another series of experiments, the heat inputs have been kept constant at 800 W, and the inlet liquid temperature varied between −10 and 23 °C. Results obtained from the experimental work have been used to validate the modeling approach (Table 4).

During the pressure-drop type oscillations, the mass flow rate, heat transfer coefficient, and heat input into the fluid keep changing. However, the heat generated in the heater wall by the electric current is constant. Therefore, when the limit cycle enters the liquid region, the wall temperature decreases as the liquid heat transfer coefficient is usually high; whereas when the limit cycle enters the vapor region, the wall temperature increases. Thus, the wall temperature keeps fluctuating during the limit cycle. These are termed as the thermal oscillations.

#### 4.8.1. Governing equations

(a) Rate of heat transfer into the fluid

$$Q_l = \int_{A_h} h(T_w - T_f)dA \tag{21}$$

The heat transfer coefficient $h$ in Eq. (21) is to be calculated under oscillating conditions, and is obtained from the following correlation [19]:

$$\mathrm{Nu} = 190C_S\left(\frac{P}{P_C}\right)^{0.25}\left(\frac{qd_e}{h_{lv}\mu_l}\right)^{0.7}e^{-0.125x} \tag{22}$$

where $\mathrm{Nu} = hd_e/k_l$, $h$ is the local heat transfer coefficient, $d_e$ is the effective diameter of the heater tube, $k_l$ is the saturated liquid thermal conductivity (= 1 for bare tube), $C_s$ is the dimensionless surface condition coefficient, when the tube is coated (Union Linde High Flux coating), and $q$ is the heat flux density.

The heater wall temperature can be calculated from the energy balance for the heater, yielding

$$\frac{d(T_w)}{dt} = \frac{Q_O - Q_l}{m_h c_h} \tag{23}$$

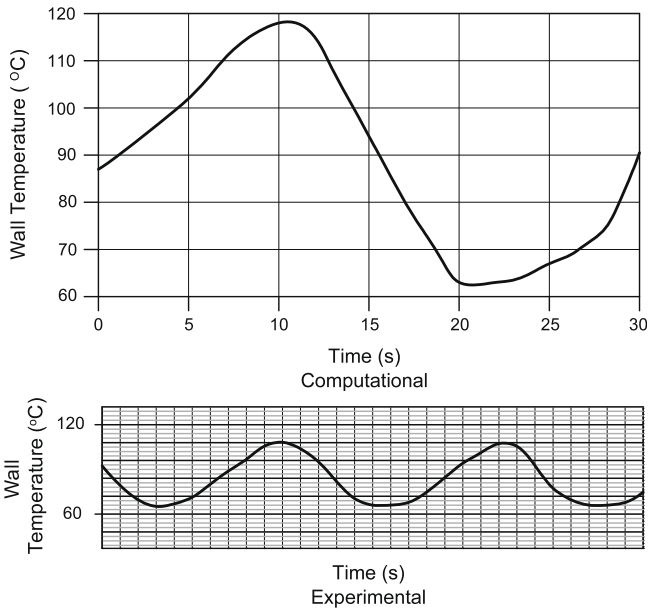


**Fig. 9.** Thermal oscillations in horizontal two-phase flow ($Q$ = 2000 W, $G$ = 0.0392, $T_i$ = 16 °C).

**Table 4**
Comparison of experimental and theoretical results for the vertical system (heater tube; nichrome with I.D. = 7.5 mm and O.D. = 9.5 mm).

| Heater tube surface | Inlet temperature (°C) | Mass flow rate (g/s) | Heat input (W) | Mass flow rate (g/s) | Experimental | | Theoretical | |
|---|---|---|---|---|---|---|---|---|
| | | | | | Period (s) | Amplitude (bar/°C) | Period (s) | Amplitude (bar/°C) |
| Coated | 23 | 7.31 | 800 | Heater inlet pressure | 50 | 0.96 | 57 | 0.94 |
| | | | | Heater inlet temperature | 50 | 99.8 | 57 | 96.0 |
| Coated | 23 | 11.89 | 800 | Heater inlet pressure | 28 | 0.89 | 27 | 1.14 |
| | | | | Heater inlet temperature | 28 | 65.6 | 27 | 75.0 |
| Bare | 23 | 7.31 | 600 | Heater inlet pressure | 25 | 0.50 | 30 | 0.69 |
| | | | | Heater inlet temperature | 25 | 49.2 | 30 | 40.0 |
| Coated | 0 | 7.31 | 800 | Heater inlet pressure | 60 | 1.06 | 59 | 0.98 |
| | | | | Heater inlet temperature | 60 | 132.1 | 59 | 122.0 |

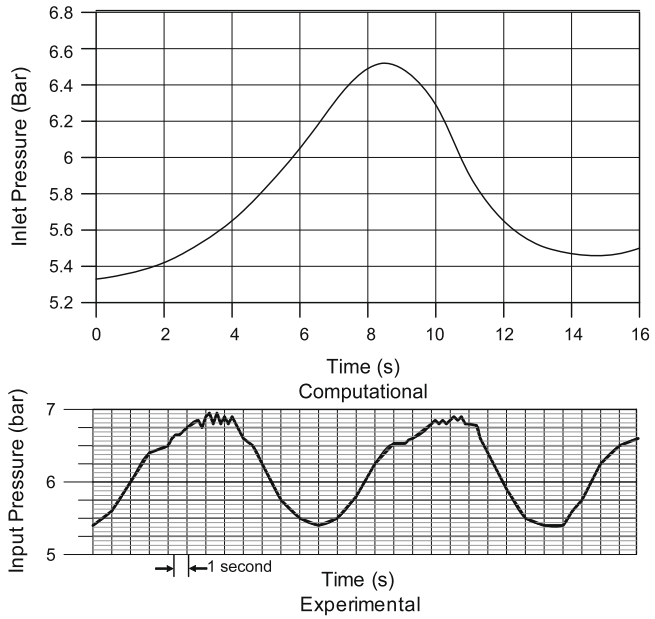


**Fig. 10.** Pressure-drop type oscillations in horizontal two-phase flow ($Q = 800$ W, $G = 0.0717$ kg/s, $T_i = 16$ °C).

In the pressure-drop oscillation model, fluid parameters and properties are calculated along the system during the oscillations. The fluid temperature inside the heater at any node is known. The heat transfer coefficient is calculated using Eq. (22). To start with, the heat input into the fluid is assumed. Then the heater wall temperature can be calculated. During the oscillations, the heat transfer coefficient and the heat input change, and the heater wall temperature changes accordingly.

The solutions of these equations, which are coupled with the hydraulics of the system, as described earlier, yield the thermal oscillations at any node of the heater. Table 4 summarizes the comparison between the experimental and theoretical results, Padki et al. [15].

*4.8.2. Time dependent results for horizontal system*

Figs. 9–12 show typical recordings of pressure-drop and thermal oscillations occurring in the horizontal flow system [16,17]. In Figs. 9 and 10, a comparison between theoretical model and experimental results are presented. Fig. 9 shows results the pressure-drop oscillations in horizontal two-phase flow, obtained for the exit restriction diameter equals to 2.616 mm, and the tube diameter 10.90 mm. The heat input to the fluid in this case is 2000 W, with Refrigerant as the working fluid. The mass flow rate for the results shown in Fig. 9 is 0.0392 kg/s; and fluid inlet temperature is 16 °C. In Fig. 10, the diameters of the exit restriction and the tube are 2.64 and 10.90 mm, respectively. The heat input to the fluid is 2000 W and the mass flow rate is 0.0717 kg/s, with R-134A as working fluid.

It is seen that the pressure-drop type and thermal oscillations are slightly out of phase with each other. The rising portion of the pressure-drop oscillations corresponds to an increasing vapor flow that carries away more heat, thus lowering the wall

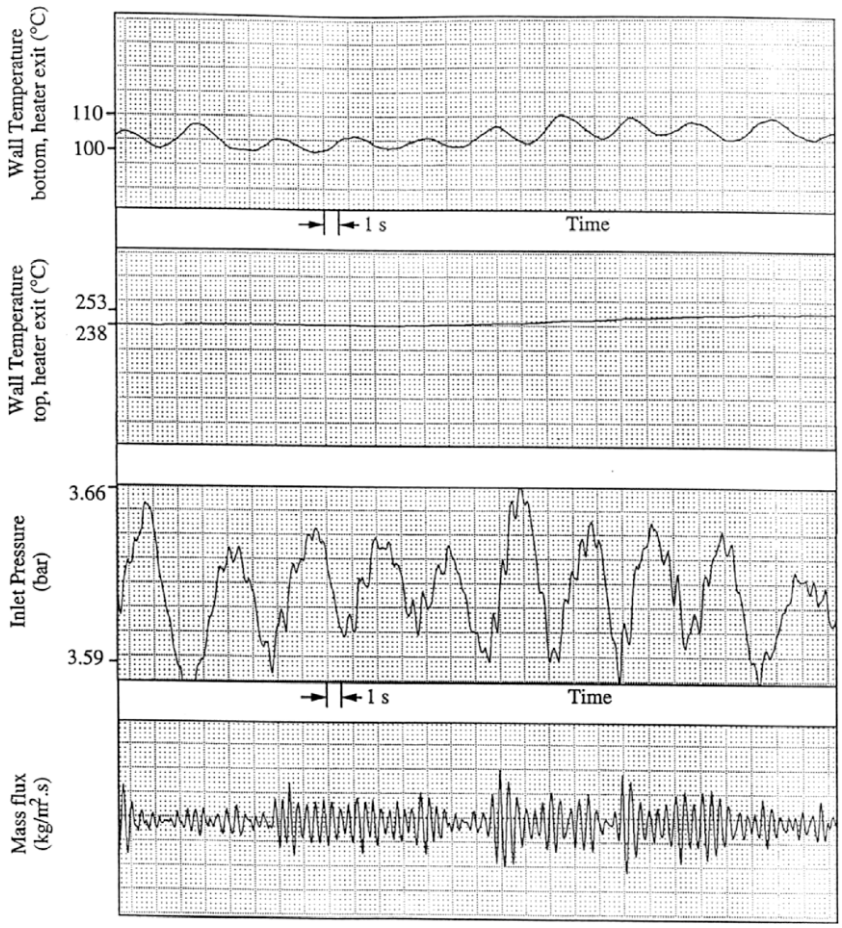


**Fig. 11.** Thermal oscillations at bottom wall ($G = 90$ kg/m$^2$ s, $T_i = 24$ °C, $\beta = 0.24$, $q = 68.3$ kW/m$^2$).

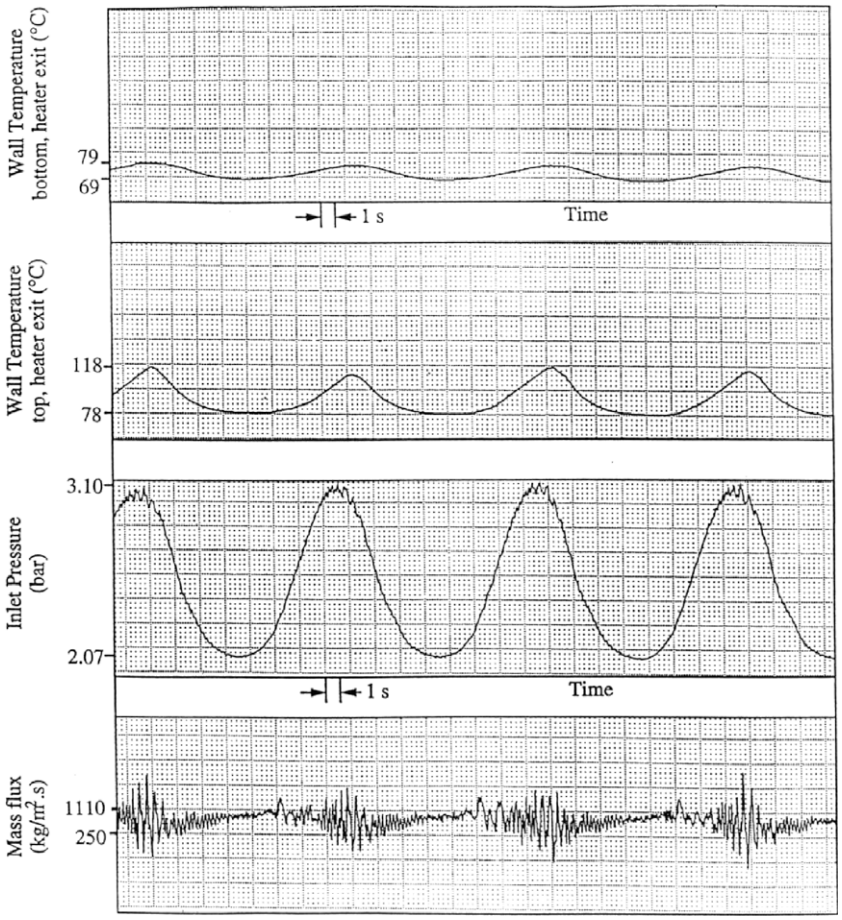


**Fig. 12.** Pressure-drop type oscillations ($G$ = 680 kg/m$^2$ s, $T_i$ = 24 °C, $\beta$ = 0.30, $q$ = 54.6 kW/m$^2$).

temperature. The decreasing portion corresponds to a decreasing liquid mass flow rate that transfers progressively lower heat away from the wall. This causes the temperature to increase. The experimental and theoretical results exhibit this characteristic clearly and are themselves in good agreement. Details of the numerical solutions are outlined in [17].

The experimental cases are selected so that at least two different cases of relevant parameters are represented, i.e., operating mass flow rate, heat input, inlet subcooling, and the heater surface condition. It can be seen that there is good agreement between the two. The periods, amplitudes, as well as the waveforms, of the oscillations are reasonably well predicted by the theory. Tables 5 and 6 summarize the comparison between the experimental and theoretical results [17].

**Table 5**
Comparison of results from the Drift-Flux model and experimental studies. Steady-state characteristics, horizontal single channel, working fluid: R-11, I.D. = 8.34 mm, and O.D. = 10.6 mm, exit restriction = 2.64 mm.

| Mass flow rate (kg/s) | Heat input (W) | Experimental pressure-drop (bar) | Theoretical pressure-drop (bar) |
|---|---|---|---|
| 0.03 | 0 | 0.2 | 0.3 |
| 0.03 | 2000 | 4.0 | 4.1 |
| 0.03 | 2500 | 6.2 | 7.2 |
| 0.06 | 0 | 0.82 | 0.85 |
| 0.06 | 2000 | 3.7 | 3.7 |
| 0.06 | 2500 | 5.0 | 5.0 |
| 0.09 | 0 | 2.0 | 2.0 |
| 0.09 | 2000 | 3.0 | 2.7 |
| 0.09 | 2500 | 3.1 | 3.1 |

**Table 6**
Comparison of experimental and theoretical results, pressure-drop oscillations in a horizontal single channel flow, mass flow rate = 0.0717 kg/s, heater tube = 8.34 mm I.D. = 8.34 mm, and O.D. = 10.9 mm, working fluid: R-11.

| Exit restriction (mm) | Heat input (W) | Period (s) | Amplitude (bar) | Period (s) | Amplitude (bar) |
|---|---|---|---|---|---|
| 2.64 | 2000 | 18 | 1.5 | 24 | 1.9 |
| 2.64 | 2500 | 16 | 2.2 | 18 | 2.0 |
| 3.175 | 2000 | 13 | 1.1 | 12 | 1.25 |
| 3.175 | 2500 | 14 | 1.2 | 12 | 1.4 |

The pressure-drop oscillations result through the interaction between the flow and the compressible volume in the surge tank. Under the present experimental conditions, high frequency density-wave oscillations also occur, which are superimposed on the pressure-drop oscillations. The present model can predict the pressure-drop oscillations quite well. However, density-wave oscillations cannot be predicted by this model, because it does not take into account explicitly the propagation of continuity waves that generate these oscillations.

## 5. Conclusions

The Drift-Flux model is adopted in the theoretical study of the pressure-drop type oscillations in the upflow and horizontal boiling flow systems.

- A model of two-phase mixture flowing through the exit restriction is developed based on the separated flow model in conjunction with the homogeneous flow model. By comparing the model with the experimental data, it is shown that it predicts

well the experimental results of the restriction characteristics, thus can be incorporated in the modeling of the dynamic instabilities of our boiling flow system.

- Finite difference method is used in solving the governing equations to obtain the steady-state characteristics of the boiling system. The results of the theoretical models are compared with the experimental steady-state curves of the system, and it is found that the theoretical calculation fit the experiment with satisfaction.
- Both the pressure-drop type and thermal oscillations occur at all heat inputs. At a given inlet subcooling, the amplitudes and periods of the oscillations increase with increasing heat input rate.
- Both the pressure-drop type and thermal oscillations occur at all inlet subcoolings. At a given heat input rate, the amplitudes and periods of the oscillations increase with increasing inlet subcooling.
- Thermal oscillations accompany the pressure-drop type oscillations. Oscillations of pressure and temperature are in phase; but the maximum of pressure oscillations always lags as compared with the maximum of temperature oscillations.
- The period and amplitude of the oscillations increase with decreasing mass flow rate at the initial operating point on the negative slope.
- The steady-state characteristics and the oscillations predicted with the use of the Drift-Flux model are reasonably in agreement with the experimental results.

## References


[1] J.A. Bouré, A.E. Bergles, L.S. Tong, Review of two-phase instabilities, Nucl. Eng. Des. 25 (1973) 165.

[2] A.E. Bergles, Review of instabilities in two-phase systems, in: S. Kakaç, F. Mayinger, T.N. Veziroglu (Eds.), Two-phase Flow and Heat Transfer, Hemisphere, Washington, D.C., 1977, pp. 383–422.

[3] R.T. Lahey, D.A. Drew, An assessment of the literature related to LWR instability modes, NUREG/CR-1414, 1980.

[4] G. Yadigaroglu, Two-phase flow instabilities and propagation phenomena, in: J.M. Delhaye, M. Giot, M.L. Rietmuller (Eds.), Thermohydraulics of Two-phase Flow Systems for Industrial Design and Nuclear Engineering, Hemisphere, New York, NY, 1981.

[5] S. Kakaç, H. Liu, Two-phase flow dynamic instabilities in boiling systems, in: X.J. Chen, T.N. Veziroglu, C.L. Tien (Eds.), Multi-phase Flow and Heat Transfer, vol. 1, Hemisphere, Washington, DC, 1991, pp. 403–444.

[6] S. Kakaç, B. Bon, A review of two-phase flow dynamic instabilities horizontal and vertical in-tube boiling systems, Int. J. Heat Mass Transfer. Available from: <www.elsevier.com/locate/ijhmt>, 2007.

[7] A.H. Stenning, Instabilities in the flow of a boiling liquid, J. Basic Eng. Trans. ASME Ser. D 86 (1964) 213.

[8] A.H. Stenning, T.N. Veziroglu, Flow oscillation modes in forced convection boiling, in: Proceedings of Heat Transfer and Fluid Mechanic Institute, 1965, pp. 301.

[9] J.S. Maulbetsch, P. Griffith, System-induced instabilities in forced convection flow with subcooled boiling, in: Third International Heat Transfer Conference, Chicago, IL, vol. 4, 1966, pp. 247.

[10] N. Zuber, F.W. Staub, G. Bijwaard, Vapor void fraction in subcooled boiling and saturated boiling systems, in: Proceedings of the Third International Heat Transfer Conference, A.I.Ch.E., New York, vol. 5, 1966, pp. 24.

[11] N. Zuber, D.E. Dougherty, Liquid metals challenge to the traditional methods of two-phase flow investigations, in: Symposium on Two-Phase Flow Dynamics, Eindhoven, Brussels, vol. 1, 1967, pp. 1091, EURATOM.

[12] P.G. Kroeger, N. Zuber, An analysis of the effects of various parameters on the average void fractions in subcooled boiling, Int. J. Heat Mass Transfer 11 (1968) 211–232.

[13] P. Saha, N. Zuber, Point of net vapor generation and vapor void fraction in subcooled boiling, in: Proceedings of the Fifth International Heat Transfer Conference, vol. IV, 1974, pp. 175–179.

[14] S. Kakaç, T.N. Veziroglu, M.M. Padki, L.Q. Fu, X.J. Chen, Investigation of thermal instabilities in a forced convection upward boiling system, Int. J. Exp. Thermal Fluid Sci. 3 (1990) 191–201.

[15] M.M. Padki, H.T. Liu, S. Kakaç, Two-phase flow pressure-drop type and thermal oscillations, Int. J. Heat Fluid Flow 12 (1991) 240–248.

[16] Y. Ding, Experimental investigation of two-phase flow phenomena in horizontal convective in-tube boiling systems, Ph.D. Thesis, University of Miami, Coral Gables, FL, 1993.

[17] M.R. Venkatran, Numerical modeling of two-phase flow instabilities in a single channel horizontal flow systems, M.S. Thesis, University of Miami, 1993.

[18] H.T. Liu, Parametric study of two-phase flow instabilities in a force-convective boiling upflow system, M.S. Thesis, University of Miami, Coral Gables, FL, 1989.

[19] T. Dogan, S. Kakaç, T.N. Veziroglu, Analysis of forced boiling flow instabilities in a single-channel upflow system, Int. J. Heat Fluid Flow 4 (1983) 145–156.

[20] L. Cao, Dynamic simulation of pressure-drop type instabilities in a two-phase upflow boiling system, Ph.D. Thesis, University of Miami, Coral Gables, FL, 2000.

[21] L. Cao, S. Kakaç, H.T. Liu, P.K. Sarma, The effects of thermal non-equilibrium and inlet temperature on two-phase flow pressure-drop type instabilities in an upflow boiling system, Int. J. Thermal Sci. 39 (2000) 886–895.

[22] D. Chisholm, Two-phase flow through sharp-edged orifices, J. Mech. Eng. Sci. 19 (3) (1977) 128–130.

[23] M. Ishii, N. Zuber, Thermally induced flow instabilities in two-phase mixtures, in: Proceedings of the Fourth International Heat Transfer Conference, Paris, Elsevier, Amsterdam, 1970, Paper No. B5.11.

[24] M. Ishii, Thermally induced flow instabilities in two-phase mixtures in thermal equilibrium, Ph.D. Thesis, School of Mechanical Engineering, Georgia Institute of Technology, Atlanta, GA, 1971.

[25] N. Zuber, J. Findlay, Average volumetric concentration in two-phase flow system, J. Heat Transfer 87C (1965) 453.